Transaction F: Nanotechnology
Vol. 17, No. 2, pp. 122–132

Invited Paper

SCIENTIA IRANICA

Synthesis and Application of Silica Aerogel-MWCNT Nanocomposites for Adsorption of Organic Pollutants

H. Bargozin[1], L. Amirkhani[1], J.S. Moghaddas[1,*] and M.M. Ahadian[2]

Abstract. *Silica aerogel-multi wall carbon nanotube composites were synthesized successfully with a waterglass precursor and an ambient pressure drying method. Pure silica aerogels are so fragile that they cannot be used easily. Carbon nanotubes (MWCNT) were used as reinforcements to strengthen the mechanical properties of pure silica aerogels. Results show that inserting small amounts of MWCNT causes silica aerogels to monolith. By addition of MWCNT, monolith nanocomposites were produced with 800 m^2/g surface area and a 140° contact angle. Results show that the silica aerogels and reinforced composites have an excellent adsorption property for the removal of organic pollutants from water. The average adsorption capacity was about 5 times the composite weight for benzene, toluene, n-Hexane, kerosene, gasoline and petroleum. The adsorption isotherm was type IV for pure silica aerogels and nanocomposites, which is ideal for excellent adsorbency. Addition of MWCNTs will not decrease the pollutant adsorption capacity of the aerogels. TEM, SEM, FTIR, contact angle, BET, BJH and the porosity of pure silica aerogels and nanocomposites are measured and reported. Adsorption isotherms show that synthesized adsorbents obey the Freundlich isotherm equation.*

Keywords: *Silica aerogel; MWCNT; Nanocomposite; Adsorption; Organic pollutants; Isotherm.*

INTRODUCTION

In recent years, silica aerogels with a nanostructure matrix have increasingly attracted more attention due to their extraordinary properties and their applications to a wide variety of technological areas [1,2]. Silica aerogels have several technological applications: Cherenkov radiation detectors, radio luminescent light and power sources, thermal super insulators for windows and air conditioning systems, containers for micrometeorites and liquid rocket propellants, acoustic impedance devices, filters for automobile exhaust systems and industrial pollutants, and heterogeneous catalysis and drug delivery [3-7]. Also, these materials are ideal for pollutant adsorption, especially non-polar pollutants from water. This is due to the high amount of adsorption and ease of surface modification. This structure shows high adsorption efficiency for many different organic pollutants from water [8,9]. However, conventional synthesis of the silica aerogel have been limited by expensive starting materials, such as alkoxides and the supercritical drying process, which are not only expensive, but also dangerous and difficult to scale up [10-14]. Recently, the successful and cost effective production of silica aerogels by use of inexpensive precursors, such as sodium silicate (waterglass), using the ambient pressure drying method, has been achieved [9,10,15-19]. However, due to the weak strength resulting from high porosity and cracking along the drying process, silica aerogels cannot be applied easily to conventional applications, such as wastewater treatment [11,16,19]. Incorporating aerogels in any commercially available fibrous supporting materials, such as fiberglass, glass wool and cotton wool, is quite effective in increasing the mechanical properties. There is some research on the

1. *Transport Phenomena Research Center (TPRC), Faculty of Chemical Engineering, Sahand University of Technology, P.O. Box 51335-1996, Iran.*
2. *Institute for Nanoscience and Nanotechnology (INST), Sharif University of Technology, Tehran, P.O. Box 11365-11155, Iran.*
*. *Corresponding author. E-mail: jafar.moghaddas@sut.ac.ir*

Received 6 June 2010; received in revised form 21 September 2010; accepted 13 December 2010

synthesis of silica aerogel composites for their application in the fields of insulation and catalysts, but there is little investigation regarding the usage of aerogel-fiber matrix composites in wastewater treatment. Kim et al. synthesized flexible silica aerogel composites by compositing glass fiber and silica aerogel from different volume ratios of colloidal silica sol and TEOS-based sol. They concluded that aerogel composites from a mixture of silica sols of colloidal silica and TEOS-based silica sols showed smaller density, higher porosity and greater surface area [3]. Zhang et al. prepared hydrophobic silica aerogel-fiber composites at ambient pressure [20]. The polypropylene nonwoven fibers were distributed inside the silica aerogels as a composite to act as a supporting skeleton, increasing the mechanical property of the silica aerogels. They showed that the silica aerogels dispersed uniformly and maintained at high porosity in the aerogel-fiber composites. They found that the as-prepared silica aerogel and aerogel-fiber composites have better adsorption capacities, compared with activated carbon fiber and granular activated carbon [20]. MWCNTs have great mechanical properties and strength that are nanoscale and can easily disperse in nanopores of silica aerogels. They have a greater surface area (about 300 m^2/g), so a very small amount of them can be dispersed in all the volume of silica aerogel. MWCNTs produce a stable composite without changing the nanostructure of silica aerogels. In the present research, we synthesized and characterized in the silica aerogel and silica aerogel-MWCNT composites (MWCNT: $> 95\%$ purity) with a waterglass precursor, using an ambient pressure drying method, and surveyed their adsorption properties.

EXPERIMENTAL

For preparation of silica aerogels, sodium silicate (waterglass) with 1.35 specific gravity, containing a SiO_2:Na_2O molar ratio of 1:3.3, ammonium hydroxide, *n*-Hexane, isopropyl alcohol (IPA) and TMCS from Merck were used. For ion exchanging of sodium silicate, Amberlite IR-120 H^+ was used. For nanocomposite preparation, multi wall carbon nanotubes (from the Research Institute of the Petroleum Industry, Iran) were used. The silica hydrogels were prepared using the waterglass as the silica source. First, the waterglass was diluted with the triple deionized water (waterglass: deionized water volume ratio=1:4). Further, for replacing Na^+ with H^+ ion, the solution was stirred with an Amberlite ion exchange resin. Before ion exchanging, the solution pH was ~ 12 and subsequently became 2-3. The hydrogel was prepared by controlled addition of the NH_4OH solution (1 M) to the silica precursor, which was obtained by the ion exchange of sodium silicate. The amount of the NH_4OH solution was adjusted until the pH of the solution became 4. The sols were transferred into Teflon vessels and were aged under airtight conditions until gelation occurred. After gelation, the hydrogels were aged for 3 h in airtight containers. In order to reduce the surface tension of the pore water, the gels were kept in IPA for 4 h at 60°C. They were then kept in the *n*-Hexane at 60°C for 3 hr. The surface modification was carried out by adding 20% TMCS to the *n*-Hexane solution for 2 h at 60°C to accomplish the modification step. The modified wet gels were dried at room temperature for 10 hr; 50°C for 2 h and 200°C for 2 hr. To prepare the aerogel-MWCNT nanocomposite, an ultrasonic mixer (Bandelin ultrasonic homogenizer) was used to disperse 0.05 grams of MWCNT in 12 cc diluted waterglass before ion exchanging, and the other steps were repeated as done for silica aerogel synthesis. The power of the mixer was 70 watt, and the MWCNT solutions were mixed for 15 minutes.

The thermal stability of the hydrophobic silica aerogels, in terms of the retention of hydrophobicity, was observed using thermal analysis (TG-DTA) (Pyris Diamond, from Perkin Elmer Co). The surface area was determined by BET (BEL) analysis from the amount of N_2 gases adsorbed at various partial pressures. The pore size distributions were measured using the Barrett Joyner Halenda (BJH), (BEL) cumulative pore volume method. The bulk density of the aerogels was calculated using a microbalance scale (10^{-5} g precision) and a coulisse. The hydrophobicity of the aerogels was tested by measuring the contact angle (θ) using the Sessile method (OCA15 plus, from the Dataphysics company). The morphology and pore structure of the pure silica aerogels and composites were characterized by scanning electron microscopy (SEM, from Tescan company model TS5136MM). The mechanical properties of the samples were determined by the compression test (DIN EN ISO 604). The Transmission Electron Microscopy (TEM) image was obtained by using Philips CM120, operating at an acceleration voltage of 80 kV. The TEM samples were prepared by dispersing aerogels into a copper grid coated with an amorphous carbon film. The adsorption capacity of pure silica aerogel and MWCNT-silica aerogel nanocomposites was determined for different pollutants: benzene, toluene, *n*-Hexane, kerosene, gasoline and petroleum. Direct contact of the adsorbent with the pure adsorbents to determine their weight change and the mixing of determined amounts of adsorbents with standard solutions in the batch systems were undertaken for measuring the adsorbents capacity. In the batch system, results were confirmed using optical characterization of the water before and after treatment for some of the pollutants using a UV-Vis spectrometer (PU8755, Philips). For this purpose, first, the standard solutions were prepared, and the instrument was calibrated.

CHARACTERIZATION

Hydrophobicity is important as an indicator in the adsorption of non-polar pollutants from water. The contact angles for pure silica aerogel and the MWCNT nanocomposites are shown in Figure 1. Samples show very good hydrophobicity (above 140°), which is necessary for the adsorption of non-polar pollutants. Because the silica aerogels completely cover the MWCNTs, and MWCNTs have no effect on the preparation reactions of silica aerogels, the hydrophobicity of MWCNT-silica aerogels is very similar to pure silica aerogels.

As seen in Figure 2a, the SEM picture shows that pure aerogels have a nanoporous structure.

Multiwall carbon nanotubes were well dispersed in the silica aerogel structure. MWCNTs have a reinforcement effect on fragile silica aerogels and cause them to strengthen, because the carbon nanotubes have great strain resistances. Also, synthesis steps and materials have no effect on MWCNTs. The TEM image of MWCNT-silica aerogels is shown in Figure 3. As seen, the carbon nanotubes bonded with each other and the silica aerogels adhered to the surface of the carbon nanotubes. This caused a good reinforcement effect and prevented silica aerogels cracking in the production process (Figure 2b).

N_2 adsorption-desorption isotherms at 77 K and the pore-size distribution have been given in Figure 4. The specific surface area for pure silica aerogels is 579 m^2/g and, for MWCNT-silica aerogels, a surface area of 802 m^2/g has been obtained. The surface area of the MWCNTs themselves is about 300 m^2/g. The results show that the addition of MWCNTs to the silica aerogels precursor causes the total surface area to increase. The part of the BET curve, which has been specified as a tail in Figure 4, belongs to MWCNTs in the silica aerogel matrix. This is characteristic of samples with two or more types of surface with different energies of adsorption [21].

Adsorption isotherms are type IV and this is characteristic of a material that contains mesoporosity and has a high energy of adsorption. These often contain hysteresis attributed to the mesoporosity [21]. A sloping adsorption branch and a nearly vertical desorption branch identify pores with narrow and wide sections and interconnecting channels.

A positive deviation in the intermediate to high end of the plot in Figure 4, due to pore filling, is usually

Figure 1. Contact angle measurement for the (a) pure silica aerogel, and (b) silica aerogel-MWCNT nanocomposite.

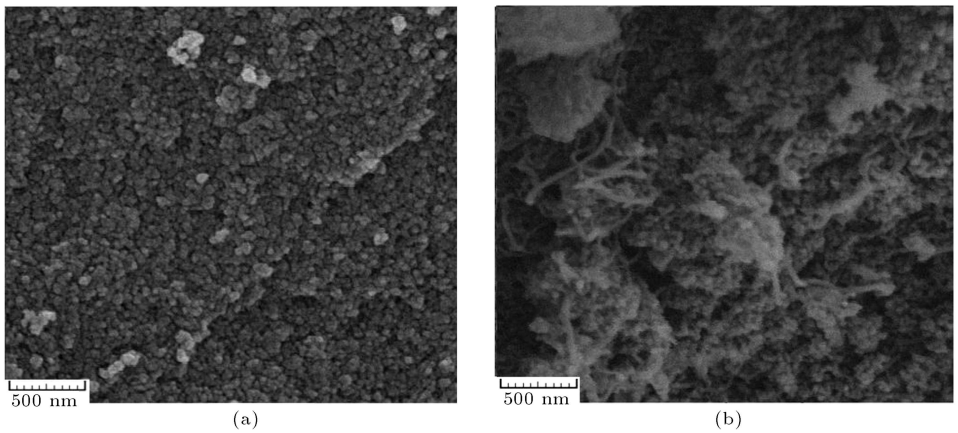

Figure 2. The SEM pictures of (a) pure silica aerogel, and (b) silica aerogel-MWCNT nanocomposites.

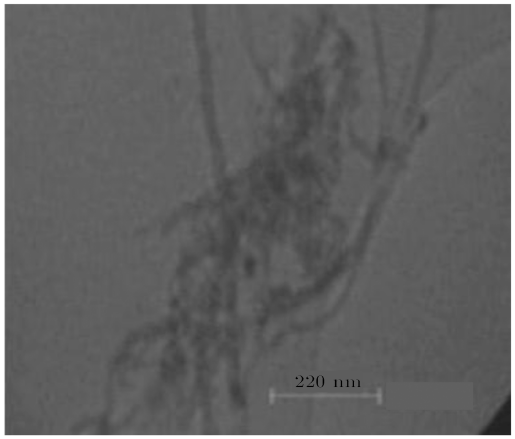

Figure 3. TEM image of MWCNT-silica aerogels.

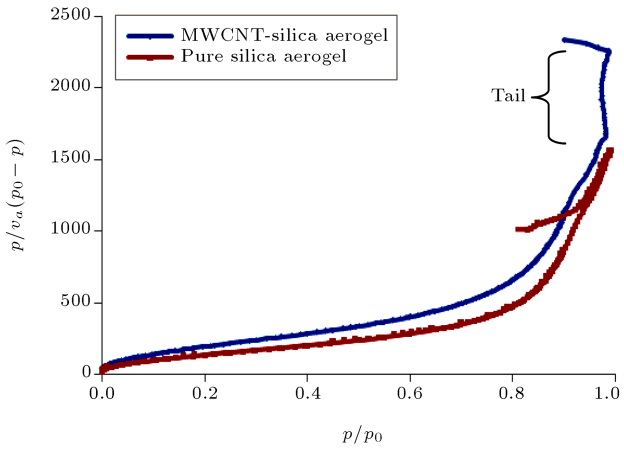

Figure 4. BET plot for pure silica aerogels and MWCNT-silica aerogels.

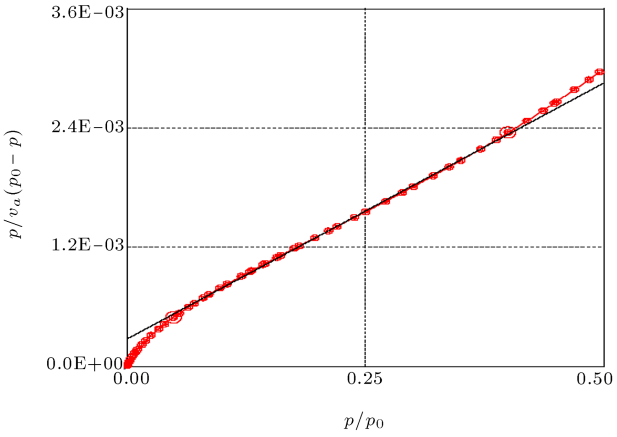

Figure 5. Transformed BET plot to determine surface; linear range is 0.05-0.35 of p_0.

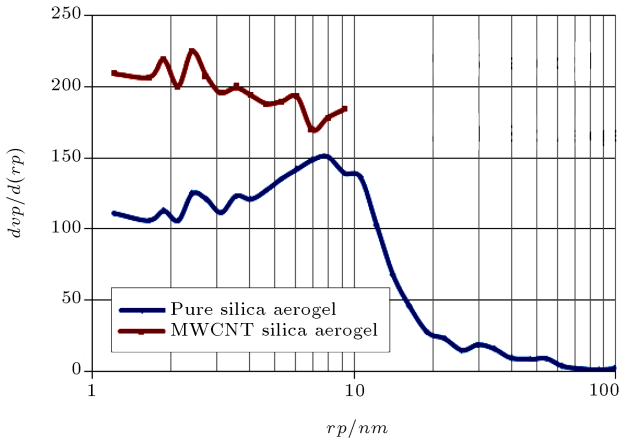

Figure 6. Pore size distribution of silica aerogels by BJH analysis.

referred to as capillary filling, which is for mesopores that exist in MWCNT-silica aerogel composites and pure silica aerogels [21].

The BET isotherm equation, for the surface area, has a restriction over the range in which the fit is valid. This range is unfortunately a matter of judgment, and phrases such as "over the linear range" have often been used in the literature. There has been a general agreement to use a saturation pressure range of 0.05-0.35, which is the pressure one would observe over the bulk liquid, p_0, for the BET equation. In the case of the BET, a linear portion of the curve for the high-energy surfaces is at about 0.05-0.35 of p_0 [21]. As seen from Figure 5, the transformed BET plot for the MWCNT-silica aerogel composite shows very good linearity at 0.05 to 0.35 p/p_0, which shows that the BET plot can be used with good accuracy.

Pore volume and pore size were analyzed by the BJH method (BEL). The nitrogen adsorption and desorption method can be applied to pores whose sizes are in the range of 17-3000 A°. As shown in Figure 6, the maximum pore size distribution is at 8 nm for pure silica aerogels and 2.5 for MWCNT-silica aerogels. In addition, results show that pore size distribution is very narrow in the case of MWCNT-silica aerogels. The high surface area of MWCNT-silica aerogels is confirmed by small and narrow pore size distribution.

The use of ultrasound in composite preparation causes the smooth dispersion of nanometer size MWCNT in the gel precursor solution, so a homogenized solution was resulted. Each MWCNT in solution acted as a good active site for wet gel formation and accelerated the solid structure formation. On the other hand, adding nanometer size MWCNT reduced the ageing time of gel formation, and it was obvious from previous work that by reducing ageing time, we could control the pore size of resulted silica aerogels [21]. Then, because the ageing time was equal for pure silica aerogel and composites (3 hrs), and solid structure formation was accelerated in the presence of MWCNTs, smaller pore size and greater surface area resulted for composites, which is in agreement with Figure 6.

The properties of pure silica aerogels and MWCNT-silica aerogels have been presented in Ta-

Table 1. Physical properties of silica aerogel and nanocomposites.

	Pure Silica Aerogel	**Silica Aerogel-MWCNTT Nanocomposite**
Density (g/cm^3)	0.11	0.23
Contact Angle	143	140
Percentage of Volume Shrinkage	5	25
Pore Size (nm)	8 nm	2.5 nm
Surface Area (m^2/g)	579	802
Total Pore Volume (cm^3 g^{-1})	2.38	3.6
Mean Particle Diameter (nm)	16.5	18

ble 1. In addition, greater particle size, in the case of composites, have confirmed the previous discussion about MWCNTs effect on the ageing time.

For obtaining hydrophobic silica aerogels, the -OH groups on the surface of aerogels must be exchanged with hydrophobic ones, such as -CH_3 groups in TMCS. Figure 7 shows the FTIR spectra (PU 9800, from Philips) of modified silica aerogels with TMCS. The transmittance peaks near 3,500 cm^{-1} are due to -OH groups, which is obvious in the xerogel sample, and which disappear for modified gels. Broad absorption bands between 1,200 cm^{-1} are due to Si-O-Si asymmetric stretching, and bending vibrations. The peak at 1,630 cm^{-1} represents the Si-OH stretch vibrations in the xerogel sample, which disappears in pure modified silica aerogels and MWCNT-silica aerogels. The light peak at the range of 1600-2200 cm^{-1} and 2600-3200 represents the characteristic stretching vibrations of C=C bonds related to the expected multiwall carbon nanotubes, which is not obvious in modified pure silica aerogels.

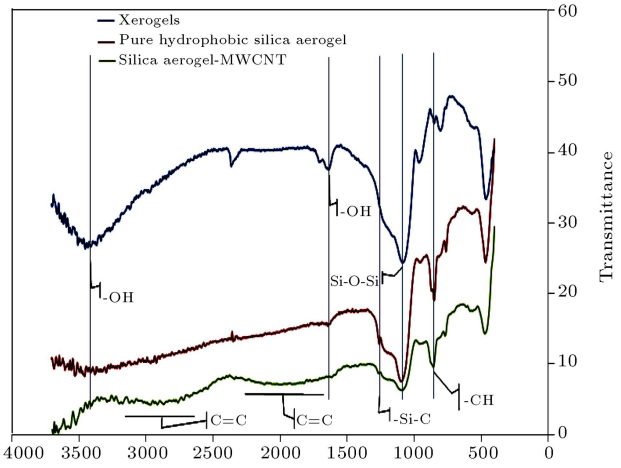

Figure 7. Surface chemical bonds detection by FTIR.

Figure 8 shows the pure silica aerogels and nanocomposites synthesized in this work and Table 1 shows the physical properties of pure silica aerogels and nanocomposites.

The compression test was used for determining the effect of MWCNT on the mechanical properties of the silica 3D structure. Figure 9 shows that MWCNT nanocomposites can bear greater stress than pure ones. Figure 9 also shows that MWCNT nanocomposites are monolithic after the synthesis process (0.05 wt%

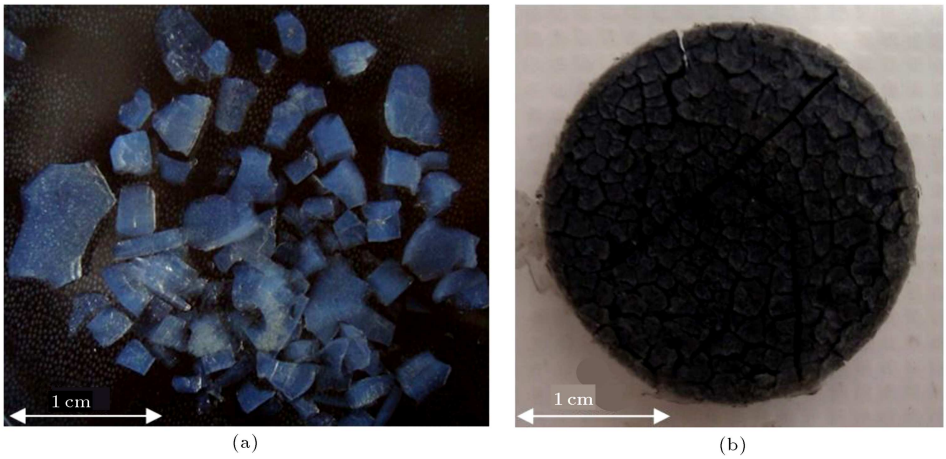

(a) (b)

Figure 8. (a) Cracked pieces of pure silica aerogels. (b) Monolith MWCNT-silica aerogel.

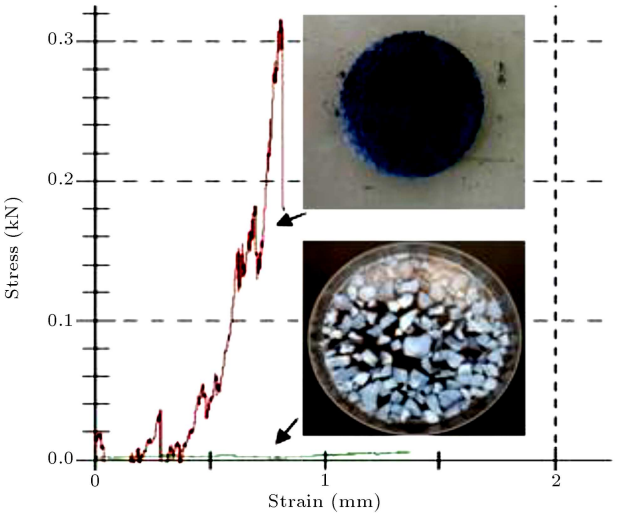

Figure 9. Mechanical strength of pure silica aerogels and MWCNT-silica composite.

MWCNT). Results show that pure silica aerogels are very fragile and cannot bear any strain, but composites can bear as much as 300 N strain pressure. This improvement in mechanical properties prevents the cracking of composite silica aerogels. Monolithic silica aerogels are much better for industrial usage, despite fragile silica aerogels.

ADSORPTION RESULTS AND DISCUSSION

The adsorption of several water pollutants, such as benzene, toluene, *n*-hexane, kerosene, gasoline and petroleum, on pure silica aerogels and MWCNT-silica aerogels is undertaken using two methods: the mass adsorption of pure pollutants and the batch adsorption of different concentrations of pollutants from water. The adsorption isotherms are calculated and results show that pure silica aerogels and MWCNT-silica aerogels have approximately similar properties and obey the Freundlich adsorption isotherm.

Mass Adsorption

In the mass adsorption method, adsorbents weight were measured with a microbalance (10^{-5} g accuracy) and to pure solutions of pollutants. After, the adsorbents were saturated with solution, drained for 2 mins and then were carefully weighted. The uptake capacity of the adsorbents was obtained using this formula:

$$\text{Uptake capacity (g adsorbate/g adsorbent)} = (m_2 - m_1)/m_1. \quad (1)$$

m_1 is the initial weight of the adsorbent and m_2 is the final weight of the adsorbent (after draining).

Table 2. Adsorption capacity of adsorbents (g adsorbate/g adsorbent).

	Silica Aerogel	Silica Aerogel-MWCNT Nanocomposites	Typical Carbon Active
Benzene	5	4.7	2.3
Toluene	7	5	1.7
Xylene	5.5	4.8	1.2
***n*-Hexane**	6.6	5.2	2.7
Kerosene	8	4.5	0.4
Gasoline	6.9	5	1.7
Petroleum	7.8	4.7	0.1

Silica aerogels easily damage because of their poor mechanical strength, while the aerogel-MWCNT composites are more applicable because their mechanical strength has considerably improved. MWCNTs have extremely tensile properties, and because of good dispersion in the precursor solution, prevent silica aerogels from cracking in the drying step. Table 2 shows the adsorption capacity for synthesized adsorbents and typical active granule carbon under the same conditions for different adsorbates. Results show that the adsorption capacity ratio of composites to active carbon is 2 times for *n*-Hexane and 47 times for petroleum.

Batch Adsorption

The adsorption capacity from water was also measured using optical characterization of the water before and after treatment, using a UV-Vis spectrometer (PU8755, Philips). For this purpose, first, the standard solutions were prepared and the instrument was calibrated.

ADSORPTION KINETIC EXPERIMENTS

This experiment was done at 20°C. 0.02 g of the adsorbent was added in a 100 mL conical flask containing a 80 cc standard solution of pollutants with a concentration of 60 mg/l. The solutions were mixed by a magnet mixer at 500 rpm. Figure 10 shows the adsorption kinetics of BTX compounds. The uptakes attained equilibrium at approximately 1 h. In order to present an equation representing kinetic adsorption, two mechanisms; pseudo-first-order and pseudo-second-order equations, were used. The pseudo-first-order equation is expressed as follows:

$$\frac{dq_t}{dt} = k_1(q_e - q_t). \quad (2)$$

Taking into account the boundary conditions $t = 0$ to $t = t$ and $q = 0$ to $q = q$, the integrated form of

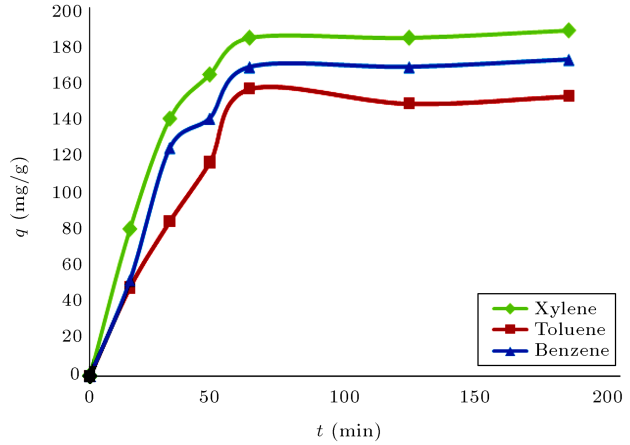

Figure 10. Adsorption kinetics of BTX compounds.

Equation 2 can be rearranged to obtain the following equation:

$$\ln(q_e - q_t) = \ln q_e - k_1 t, \tag{3}$$

where k_1 (min^{-1}) is the rate constant of the pseudo-first-order adsorption, q_e (mg g^{-1}) is the adsorption capacity at equilibrium; and q_t (mg g^{-1}) is the adsorption capacity at time t (min).

The pseudo-second-order equation is expressed as follows:

$$\frac{dq_t}{dt} = k_2(q_e - q_t)^2, \tag{4}$$

$$\frac{t}{q_t} = \frac{1}{k_2 q_e^2} + \frac{t}{q_e} = \frac{1}{v_0} + \frac{t}{q_e}, \tag{5}$$

where k_2 (gmg^{-1} min^{-1}) is the constant of pseudo-second-order rate, and v_0 represents the initial adsorption rate (mg g^{-1} min^{-1}).

The corresponding results of parameters and correlation coefficients for the model were given in Figure 11 and Table 3.

It could be seen that the kinetics of BTX adsorption followed the pseudo second-order rate expression, showing that the adsorption rate may be controlled by the concentration of BTX and the number of active sites on the adsorbent surface. At the initial adsorption phase, the active sites were not occupied, and the adsorption rate is fast. With the occupation of these sites, the rate decreased until the final sorption-desorption equilibrium was attained.

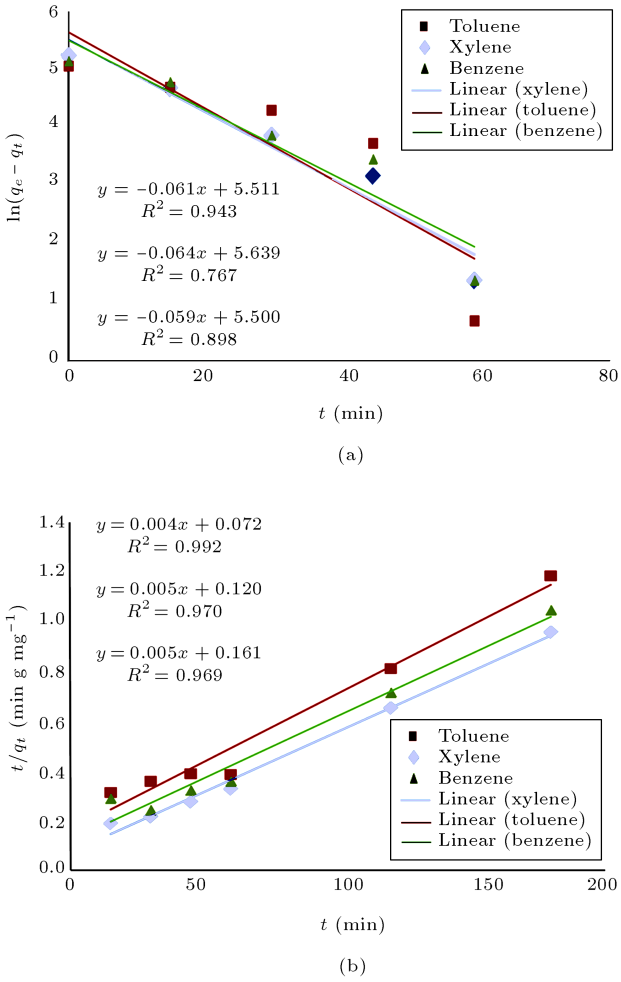

Figure 11. (a) Pseudo-first-order equation. (b) Pseudo-second-order equation for BTX adsorption.

ADSORPTION ISOTHERMS

The 80 cc standard solution of pollutants with different concentrations of 10, 20, 30, 50 and 60 mg/l were prepared and mixed for one hour with a magnet mixer at 500 rpm and 20°C for obtaining adsorption isotherms. First, the standard solutions for calibration of the equipment were prepared and the equipment was calibrated. As seen in Figure 12, the equipment was calibrated very carefully and the results are linear.

The adsorption isotherm model describes how adsorbate interacts with adsorbents, and an understanding of the nature of interaction is essential for the

Table 3. Kinetic parameters of the pseudo-first-order and pseudo-second-order equations for BTX adsorption.

	Pseudo-First-Order Equation		**Pseudo-Second-Order Equation**	
	k_1 (min^{-1})	R^2	v_0 (mg g^{-1} min^{-1})	R_2
Benzene	0.059	0.898	8.333	0.97
Toluene	0.064	0.767	6.2	0.969
Xylene	0.061	0.943	13.889	0.992

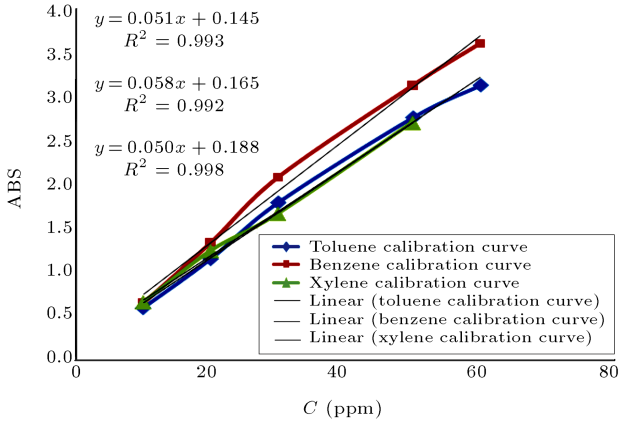

Figure 12. Calibration of UV-Vis equipment with standard solutions.

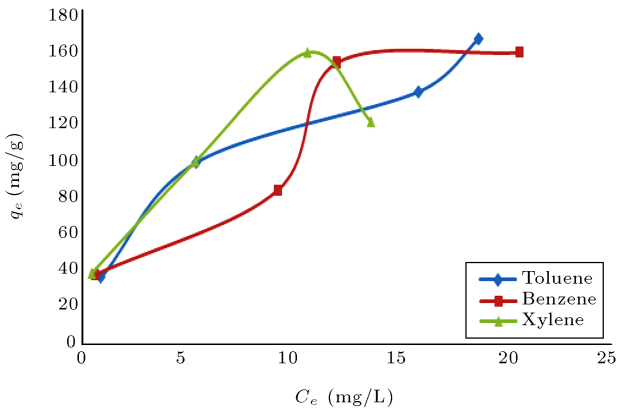

Figure 13. Adsorption isotherms for benzene, toluene, xylene at 20°C.

most effective use of the adsorbent. Thus it is essential to correlate the equilibrium data by either theoretical or empirical models for designing a perfect operating adsorption system for industrial effluents.

In this study, experimental data were modeled by the Langmuir model (Equation 6) and the Freundlich model (Equation 7).

$$q_e = \frac{q_m k_L C_e}{1 + k_L C_e}, \tag{6}$$

$$q_e = K_f C_e^{\frac{1}{n}}, \tag{7}$$

where q_e is adsorption capacity (g adsorbate/ g adsorbent), C_e is adsorbate equilibrium concentration in the liquid (mg/L), q_m and k_L are constants related to the loading capacity and the free energy of adsorption. K_f and n are Freundlich parameters, K_f is the adsorption equilibrium constant and n is constant, indicative of adsorption intensity. For a good adsorption system, we could reach a high adsorption capacity (q_m) and a low equilibrium concentration of the target compound (C_e). Thus a large K_f value and a small $1/n$ value results in a more effective adsorbent. For good adsorbents, n is always greater than 2.

The BTX adsorption isotherms at 20°C for MWCNT-silica aerogels are obtained and plotted in Figure 13.

Adsorption isotherms are modeled with Langmuir and Freundlich models, which are shown in Figure 14.

The parameters of the two equations are given in Table 4. In all cases, the correlation coefficients, R^2, for the Freundlich model, are better than the Langmuir model, indicating that the Freundlich model predicts the experimental data better.

For comparison between pure silica aerogels and MWCNT-silica aerogels, and showing the effect of MWCNTs on the silica aerogel adsorption properties, Freundlich isotherms of toluene, benzene and xylene are presented in Figures 15 to 17.

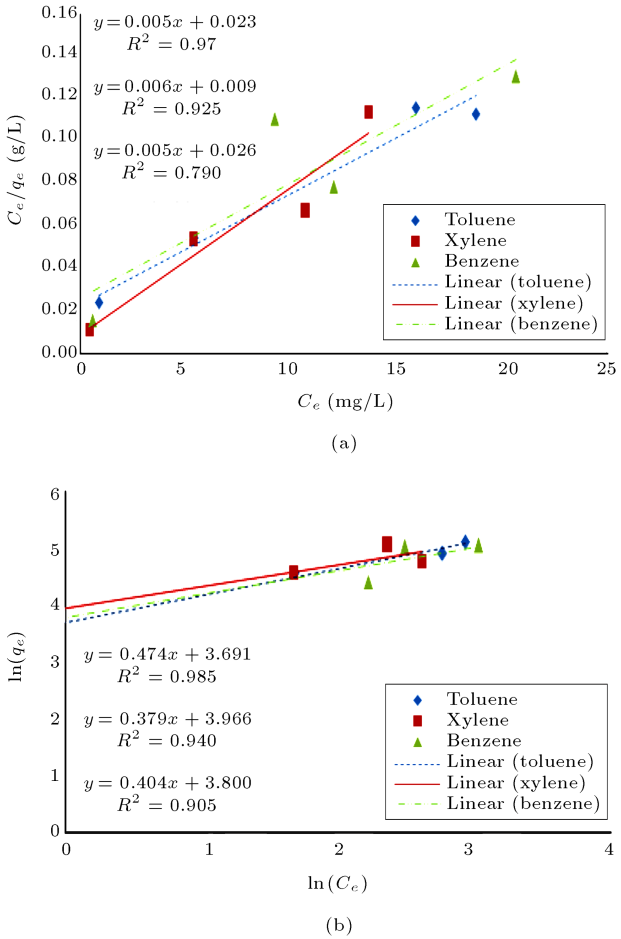

Figure 14. Equilibrium isotherms of BTX adsorption on aerogel-MWCNT composite. (a) Langmuir plots; and (b) Freundlich plots.

Results show that the addition of a small amount of MWCNT to aerogel structures does not influence the adsorption properties of silica aerogels, despite the mechanical property. The concentrations used for isotherms are chosen, such as to be in the range of solubility of the pollutants in the water at 20°C.

Table 4. Equilibrium isotherm model parameters for BTX adsorption.

	Langmuir Model			Freundlich Model		
	q_m (mg/g)	k_L (L/mg)	R^2	K_f	$1/n$	R^2
Benzene	200	0.192	0.79	44.72	0.404	0.905
Toluene	200	0.217	0.97	40.09	0.474	0.985
Xylene	166.67	0.667	0.925	52.80	0.379	0.94

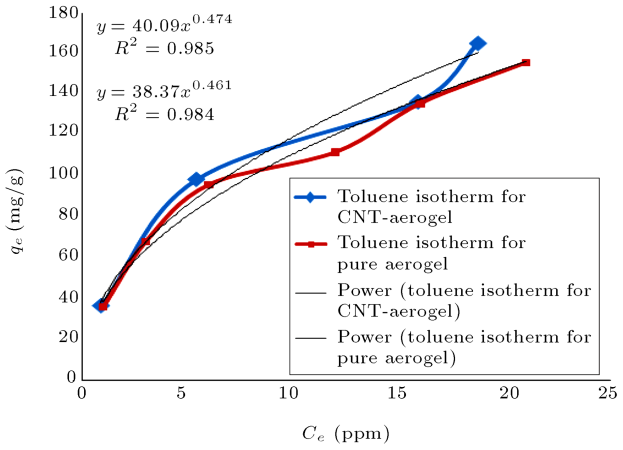

Figure 15. Toluene isotherms at 20°C for pure silica aerogels and MWCNT composites.

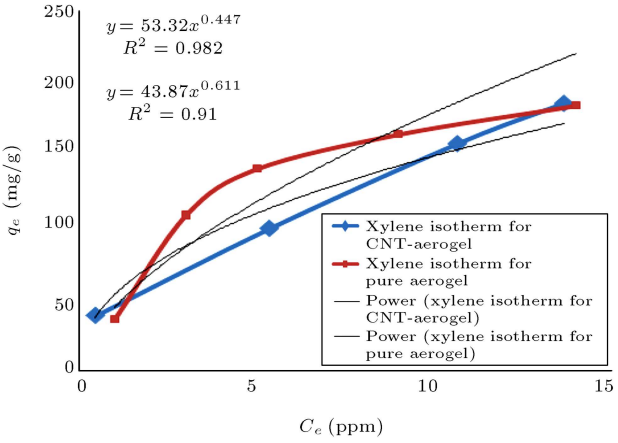

Figure 17. Xylene isotherms at 20°C for pure silica aerogels and MWCNT composites.

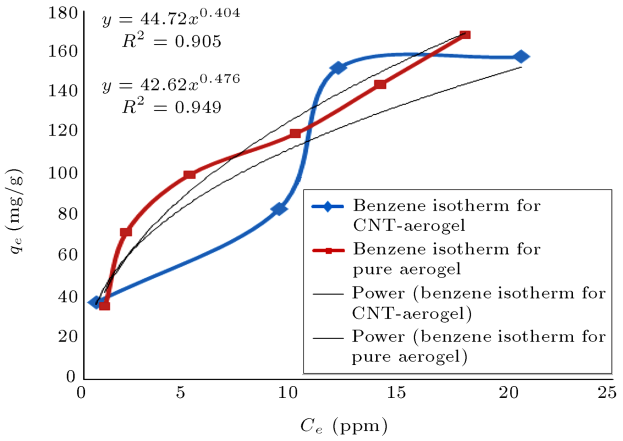

Figure 16. Benzene isotherms at 20°C for pure silica aerogels and MWCNT composites.

In Table 5, the results of modeling with Freundlich adsorption isotherms are shown. K_f and n are the parameters of the Freundlich adsorption isotherm for good adsorbents; the first must be as high as possible and the second must be greater than 2. In the case of toluene and benzene, the results are similar, but in the case of xylene, the results show that the addition of MWCNT causes the adsorption properties of adsorbents to improve.

The Freundlich isotherm equation is predicted by mesoporous adsorbents. The mechanism of adsorption in these adsorbents is that first monolayers of the adsorbate molecules are formed on the surface and then, through time, the multilayers of adsorbate are created. Because of the mesoporous size of pores, condensations of adsorbates are occurred on pores. This is the main reason for the greater adsorption capacity without volume change in adsorbents, which is confirmed by BET results. Other models of adsorption isotherm, such as Langmuir, are developed for monolayer adsorption systems. As seen from BET results, MWCNt-silica aerogels are mesoporous materials, and multilayer condensation occurs in such adsorbents.

The results in Table 4 show that the synthesized adsorbents could be easily used for pollutants adsorption from a marine environment. Marine environments, especially near onshore and offshore oil wells are polluted with greasy water from oil wells, which is emitted directly to sea water. In addition, marine pollution from oil leakages could easily be cleaned with such high

Table 5. Freundlich adsorption isotherm parameters.

Xylene			Toluene			Benzene			Adsorbent
$1/n$	n	K_f	$1/n$	n	K_f	$1/n$	n	K_f	
0.611	1.64	43.87	0.461	2.16	38.37	0.476	2.1	42.62	Pure silica aerogel
0.379	2.23	52.80	0.474	2.12	40.09	0.404	2.47	44.72	MWCNT- silica aerogel

capacity and intensity adsorbents, and because of low density, could be easily separated from the water after adsorption.

ADSORBENT REGENERATION

Adsorbents were regenerated at 150°C in an oven for one hr, several times, without a noticeable reduction in performance, but the monolithic aerogels were cracked into small pieces. In the synthesis of MWCNT-silica aerogels, surface modification with TMCS cause-CH_3 groups to be created on the surface. When adsorbents are heated to desorption with any hydrocarbon material on them, the capillary effect cause shrinkage in aerogels, but because of the existence of -CH_3 groups on the surface, after the removal of hydrocarbons, the silica aerogel shows a spring back effect and gets back to its initial volume without any reduction in performance. Also TG/DTA results (not shown here) show that MWCNT-silica aerogels can resist up to 360°C under an oxygen atmosphere, and regeneration at 150°C will not decompose the structure or reduce performance. The cracking of aerogels after several regenerations is because of thermal shocking, and by controlling the regeneration temperature, cracking could be reduced.

CONCLUSION

The synthesis and adsorption properties of MWCNT-silica aerogel nanocomposites are successfully achieved. The existence of the small amount of MWCNT in the matrix of the silica aerogel (0.05 wt%) causes it to gain a monolithic structure. The adsorption properties of the synthesized nanostructures are tested in mass and batch adsorption systems with different organic pollutants. The results indicate that the monolithic composite has an adsorption capacity of about 5 times its weight. Adsorption isotherms were obtained for toluene, benzene and xylene. Results show that nanostructured adsorbents obey the Freundlich adsorption model, and the obtained parameters of this model show that the nanostructured adsorbents have very good adsorption properties, with high adsorption capacities and intensity. As an industrial view, synthesized adsorbents have great potential in oil spill removal from the seabed. Also, the synthesis method is such that the regeneration of adsorbents could be achieved several times without any reduction in performance.

ACKNOWLEDGEMENTS

The authors wish to express their sincere gratitude to Professor A.M. Rashidi for his help in implementation of the project.

REFERENCES

1. Sub, H.I., Chul, P.J. et al. "Fabrication of the monolithic silica aerogels using sodium silicate and its network strengthening", *Key Engineering Materials*, **368-372**, pp. 790-793 (2008).
2. Dorcheh, A.S. and Abbasi, M.H. "Silica aerogel; synthesis, properties and characterization", *Journal of Materials Processing Technology*, **199**, pp. 10-26 (2008).
3. Kim, C.Y., Lee, J.K. et al. "Synthesis and pore analysis of aerogel-glass fiber composites by ambient drying method", *Colloids and Surfaces A: Physicochemical and Engineering Aspects*, **313-314**, pp. 179-182 (2008).
4. Bangi, U.K.H., Rao, A.V. et al. "A new route for preparation of sodium-silicate-based hydrophobic silica aerogels via ambient-pressure drying", *Science and Technology of Advanced Materials*, **9**, pp. 1-10 (2008).
5. Rao, A.P., Rao, A.V. et al. "Hydrophobic and physical properties of the ambient pressure dried silica aerogels with sodium silicate precursor using various surface modification agents", *Applied Surface Science*, **253**, pp. 6032-6040 (2007).
6. Hwang, S.W., Jung, H.H. et al. "Effective preparation of crack-free silica aerogels via ambient drying", *J. Sol-Gel Sci. Techn.*, **41**, pp. 139-146 (2007).
7. Bhagat, S.D., Park, K.T. et al. "A continuous production process for silica aerogel powders based on sodium silicate by fluidized bed drying of wet-gel slurry", *Solid State Sciences*, **10**, pp. 1113-1116 (2008).
8. Liu, H., Sha, W. et al. "Preparation and characterization of a novel silica aerogel as adsorbent for toxic organic compounds", *Colloids and Surfaces A: Physicochemical and Engineering Aspects*, **347**, pp. 38-44 (2009).
9. Gurav, J.L., Rao, A.V. et al. "Physical properties of sodium silicate based silica aerogels prepared by single step sol-gel process dried at ambient pressure", *Journal of Alloys and Compounds*, **476**(1-2), pp. 397-402 (2009).
10. Cha, Y.C., Yoon, J.S. et al. "Ambient pressure dried silica aerogel thin film from water glass", *Journal of the Korean Ceramic Society*, **45**, pp. 87-89 (2008).
11. Hwang, S.-W., Kim, T.-Y. et al. "Effect of surface modification conditions on the synthesis of mesoporous crack-free silica aerogel monoliths from waterglass via ambient-drying", *Microporous and Mesoporous Materials*, **130**(1-3), pp. 295-302 (2010).
12. Kim, C.Y., Lee, J.K. et al. "Characteristics of silica aerogel composites synthesized by ambient drying method", *Materials Science Forum*, **544-545**, pp. 673-676 (2007).
13. Bhagat, S.D., Kim, Y.H. et al. "Textural properties of ambient pressure dried water-glass based silica aerogel beads: One day synthesis", *Microporous and Mesoporous Materials*, **96**, pp. 237-244 (2006).

14. Kim, G.S., Hyun, S.H. et al. "Cost-effective synthesis of silica aerogels from waterglass/TEOS by ambient drying and their applications", *Ceramic Engineering and Science Proceedings*, **23**, pp. 73-78 (2002).

15. Part, Y.C., Cha, C.E. et al. "Synthesis of silica aerogel thin film from waterglass", *Diffusion and Defect Data Pt.B: Solid State Phenomena*, **124-126**, pp. 671-674 (2007).

16. Han, I.S., Park, J.C. et al. "Fabrication and network strengthening of monolithic silica aerogels using water glass", *Journal of the Korean Ceramic Society*, **44**, pp. 162-168 (2007).

17. Shi, F. and Wang, L.J. "Rapid synthesis of silica aerogels via a new ambient pressure drying process", *Dalian Ligong Daxue Xuebao/Journal of Dalian University of Technology*, **46**, pp. 241-245 (2006).

18. Lee, S., Lee, E.A. et al. "Solvents effects on physicochemical properties of nano-porous silica aerogels prepared by ambient pressure drying method", *Materials Science Forum*, **510-511**, pp. 910-913 (2006).

19. Shi, F., Wang, L. et al. "Preparation and characterization of nano-mesoporous SiO_2 aerogel via ambient pressure drying", *Kuei Suan Jen Hsueh Pao/Journal of the Chinese Ceramic Society*, **33**, pp. 963-967 (2005).

20. Zhang, X., Zhao, H. et al. "Preparation and surface modification of SiO_2 aerogel by ambient pressure drying", *Beijing Keji Daxue Xuebao/Journal of University of Science and Technology Beijing*, **28**, pp. 157-162 (2006).

21. Condon, J.B., *Surface Area and Porosity Determinations by Physisorption Measurements and Theory*, 1st Ed., USA, Elsevier (2006).

BIOGRAHIES

Hasan Bargozin was born in Iran in 1981. He received his B.S. degree in Chemical Engineering (2004) from Sharif University of Technology (Tehran) and a M.S. degree from Sahand University of Technology (Tabriz). He is now a Ph.D. student of Chemical Engineering and works in the Transport Phenomena Research Center (TPRC) in Sahand University of Technology with Prof. J.S. Moghaddas. His research is focused on Synthesis and Applications of Nanoporous Silica Aerogels with Special Application to the Wettability Alteration of Oil Reservoir Cores with Nanoporous Silica Aerogels. He is also interested in the Nanocomposites of Silica Aerogels in Upstream Oil Industry Applications. He has also worked in the Research Institute of the Petroleum Industry (RIPI) on the applications of nanotechnology to oil, gas and energy sections, as head of the nanotechnology group at the Idea Center.

Leila Amirkhani was born in Iran, in 1981. She received B.S. and M.S. degrees in Chemical Engineering from Sahand University of Technology (Tabriz) in 2003 and 2010, respectively. She is now a Ph.D. student of Chemical Engineering at the same university and works in the Transfer Phenomena Research Center (TPRC) with Prof. J.S. Moghaddas. Her M.S. thesis was about the Synthesis and Applications of Nanoporous Silica Aerogels for Adsorption of Organic Pollutants from Wastewater. She is interested in Nanocomposites of Silica Aerogels and their Applications.

Jafar Sadegh Moghaddas was born in 1966, in Iran. He is working as Associate Professor in the Chemical Engineering Department of Sahand University of Technology, Tabriz, Iran. His research interests include various areas of Mixing and Transport Phenomena in Chemical and Reservoir Engineering, including: Mixing, Applications of Silica Aerogels, EOR, Multiphase Flow, Turbulence, Bubbly Flow, Flow Visualization using Optical Methods, and Miscible Displacement of Fluids through Porous Media. He has published papers in about 30 journals and at more than 60 conferences.

Mohammad Mahdi Ahadian received a Ph.D. degree in Physics from Sharif University of Technology in 2006, where he is currently Assistant Professor at the Institute for Nanoscience and Nanotechnology (INST). His research interests include: Surface Science in addition to Synthesis, Characterization and Application Of Nanostructures.